

## Physics of GaN Devices

Michael S. Shur  
Center for Broadband Data Transport  
CII 9017, RPI, 110 8th street, Troy, NY 12180, USA  
(518) 276 2201 (phone) (518) 276 2990 (fax) shurm@rpi.edu (email)  
<http://nina.ecse.rpi.edu/shur/>

### ABSTRACT

We review the physics of GaN-based devices including pyroelectric and piezoelectric sensors, GaN-based Heterostructure Field Effect Transistors (HFETs); SAW and acousto-optics devices; UV Light Emitting Diodes, and THz plasma wave electronics devices using GaN HFETs, paying special attention to polarization effects. We also discuss oscillating electron and hole islands in semiconductor GaN or AlGaN grains embedded into a pyroelectric matrix with a larger spontaneous polarization.

### 1. INTRODUCTION

The physics of nitride semiconductor devices is quite different from that of Si-based or GaAs-based devices because nitride semiconductors have hexagonal symmetry, large bandgaps (with an exception of InN), and large polar optical phonon energies. The key difference is a large spontaneous and piezoelectric polarization in hexagonal (wurtzite) semiconductors that can induce two dimensional electron or hole gases with very high sheet densities at the heterointerfaces in nitride semiconductors. The surface electron density in GaN-based Heterostructure Field Effect Transistors (HFETs) might exceed the electron concentration in GaAs-based HFETs by a factor of 10 to 20, with a commensurate increase in the on-state current density. A wide energy gap of GaN and AlGaN results in a large breakdown voltage. As a consequence of this combination of a large current carrying capability and of a large voltage swing, GaN-based HFETs demonstrate record powers at microwave frequencies (up to 30 W/mm compared with 1 to 2 W/mm powers for their GaAs-based counterparts.) In addition, a large electron concentration in nitride semiconductor HFETs alleviates the effect of surface states, allowing for the development of insulated gate HFETs that have many additional advantages. Also, chemical inertness of nitrides makes them suitable for in vitro biological applications. Surface Acoustic Wave and pyroelectric devices are other examples, where superior properties of nitrides enable device applications.

Polarization induced fields also affect the performance of photonic nitride devices, such as deep UV Light Emitting Diodes (LEDs) and solar-blind photodetectors. Recent progress in developing deep UV LEDs has enabled applications in water and air purification and is expected to speed up the development of systems for the detection of biological hazardous agents.

Recent progress has been achieved by using AlN/AlGaN strain-defects management superlattices for defect filtration and by improved materials growth using Migration Enhanced Metalorganic Chemical Vapor Deposition (MEMOCVD). Further improvements will have to rely on better understanding of device physics, including the physics of the electron and hole transport, injection, radiative and non-radiative recombination, polarization effects, and of the low frequency noise.

A high density electron gas in nitride semiconductors supports high frequency oscillations of the electron density (called plasma wave oscillations) that lead to millimeter wave emission by GaN-based FETs at frequencies much higher than the device cutoff frequency. Polarization fields in semiconductor grains embedded into a pyroelectric matrix (for example, GaN grains in AlGaN matrix) result in the formation of quantized electronic and hole islands oscillating at terahertz frequencies. These effects (reviewed in this paper) point out to the potential applications of GaN-based devices in the terahertz range of frequencies.

The first GaN crystal synthesized in 1932 [1] with the first p-type GaN was grown only in 1961 [2], followed by the first monograph on nitrides [3] in 1969 and by the first GaN LED [4] in 1971. More recent events include the demonstration of the first GaN HEMT [5], the prediction of polarization doping [6] in 1993, the development of the first InGaN blue laser [7] in 1996, the emergence of nitride-based pyroelectric and piezoelectric devices [8], of ultraviolet Light Emitting Diodes (UV LEDs) and photodetectors [9], GaN-based high voltage HFETs and BJTs [10]

Surface Acoustic Wave and acousto-optic devices [11], and THz plasma wave electronics devices [12].

## 2. PHYSICS OF ELECTRON TRANSPORT IN InN/GaN/AlN ALLOYS

Transport properties of AlN/GaN/InN -based semiconductors have unique features compared to more conventional semiconductors, such as Si or GaAs. In these materials, the polar optical phonon energy is large (much larger than the thermal energy at room temperature). As a consequence, the dominant optical polar scattering occurs in two steps: photon absorption and re-emission (resulting in an effectively elastic scattering process). [13, 14] In high electric fields, an electron runaway plays a key role determining the peak field and peak velocity in these compounds.[15] The runaway effects are further enhanced in two dimensional electron gas at the AlGaN/GaN or AlGaN/InGaN heterointerfaces. As a result, the peak electron drift velocity and peak electric field of the 2D electrons in compound semiconductors are smaller than for the 3D electrons in these materials. [16] This prediction agrees with the results of Monte-Carlo simulations and with the measured peak velocities. In very short (e.g. sub-0.1 micron) GaN structures, ballistic and overshoot effects become important. [17] In a deep submicron structure, the ballistic effects in low electric fields reduce an apparent value of the low field mobility because of a finite electron acceleration time in the structure. A large difference between the effective masses of AlGaN and InGaN leads to a large degree of the electron wave function penetration from the 2D gas in InGaN into the AlGaN layer, which increases with an increase of the electron momentum component in the direction parallel to heterointerfaces. [18] might allow for the design of InGaN heterostructures with the breakdown voltage determined by the AlGaN breakdown field rather than by the InGaN breakdown field.

## 2. POLARIZATION INDUCED ELECTRON AND HOLE 2D GASES

Figure 1 (from [6]) shows the predicted formation of 2D hole and 2D electron gases in GaN/AlN heterostructures as a result of the screening of polarization charges.

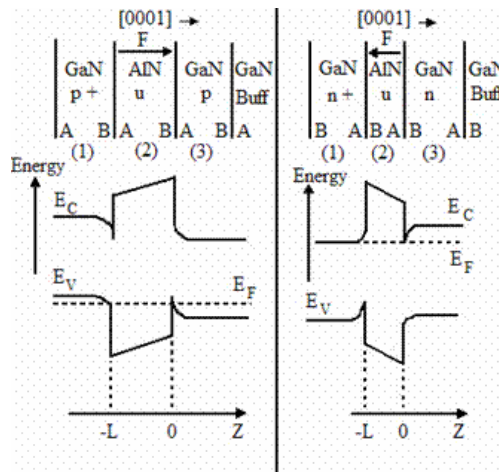


**Fig 1.** GaN-AlN-GaN SIS structures with undoped regions (marked u). A denotes cation face; B anion face. Bands crossing the Fermi level correspond to 2D gas formation [6].

Such “polarization doping” can support very large concentrations of the 2D electron gas in AlGaN/GaN HEMTs (see Figure 2.) These large carrier densities support large currents in GaN-based HFETs. In combination with a high breakdown voltage, this translates into record power levels for GaN-based HFETs from S-band to Ka-band, such as a recent report of power density of over 30 W/mm [19]. They also enable a variety of pyroelectric and piezoelectric devices [8].

## 3. PYROELECTRIC AND PIEZOELECTRIC DEVICES

GaN pyroelectric voltage coefficients are comparable to those of the pyroelectric ceramics. GaN and related materials are well suited for use in pyroelectric sensing elements at elevated temperatures, above the temperature range of traditional pyroelectric materials. Fig. 3 shows relative changes in the GaN sample resistance as a function of strain for the dynamic piezoelectric effect in GaN. This figure compares the experimental results for GaN with those for GaAs. [20] This comparison shows that n-type GaN based electromechanical sensors are more

sensitive than those made from GaAs or SiC.

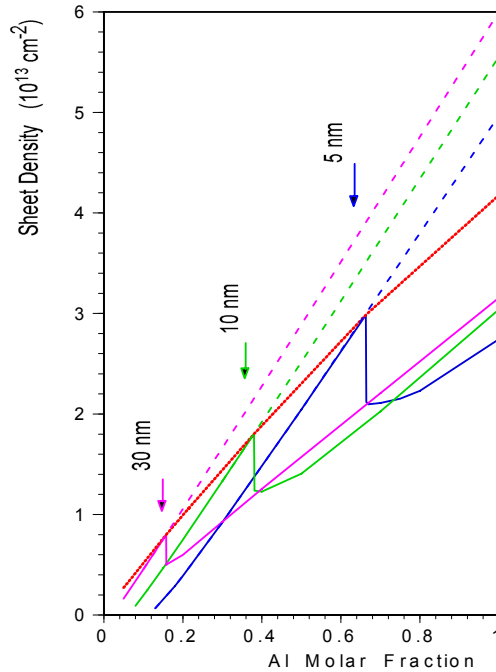


Fig. 2. Electron sheet density, induced by polarization in AlGaN-GaN heterostructures. Arrows show the onset of strain relaxation. Dashed lines correspond to unrelaxed heterostructures (from [8].)

The GaN sensors can be used for time-dependent measurements of vibrations, sudden changes in acceleration, force, pressure, etc. at frequencies higher than 1 Hz.

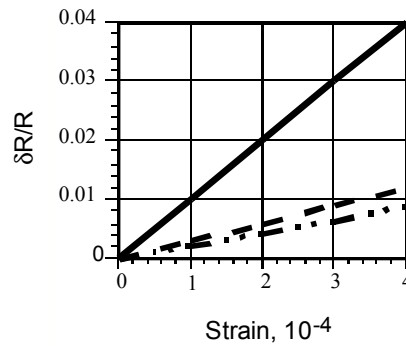


Fig. 3. Relative change in resistance versus strain for GaN (solid line) [20], SiC (dashed line) [21], and GaAs (dashed-dotted line) [22]

Fig. 4 shows a typical response of a GaN pyroelectric sensor [23]. Much (if not most) of the work in this area remains to be done and we expect future dramatic improvements in GaN-based pyroelectric sensors.

#### 4. ELECTRON AND HOLE ISLANDS IN PYROELECTRIC-SEMICONDUCTOR GRANULAR SYSTEMS

Spontaneous pyroelectric polarization induces strong built-in electric field in pyroelectric-semiconductor granular systems (pyroelectric grains in a semiconductor matrix or semiconductor grains in a pyroelectric matrix, see Fig. 5 [24]). GaN grains in an AlGaN matrix are an example of such a system.

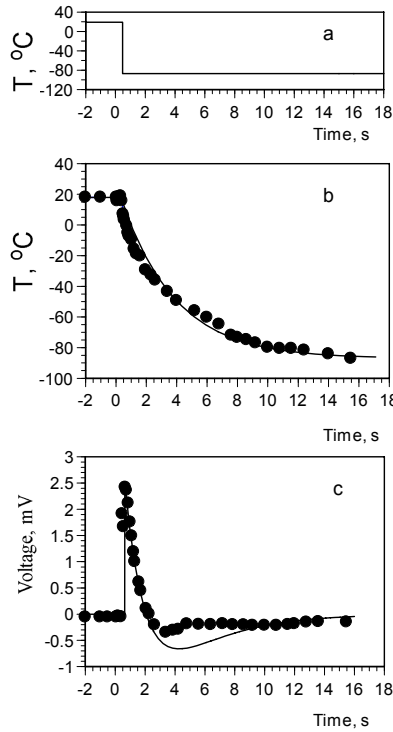


Fig. 4. Bath temperature (a), sample temperature (b), and pyroelectric voltage (c) versus time. Dots are measured data; solid curves are calculated (after [23].)

At some critical value of the grain radius, the built-in voltage drop across the grains becomes larger than the energy gap. In an intrinsic semiconductor, two moveable (electron and hole) islands appear at the grain surface. The plasma oscillations of such islands correspond to the terahertz range of frequencies. In an *n*-type semiconductor, the depletion and accumulation regions are formed due to a built-in electric field. [25]

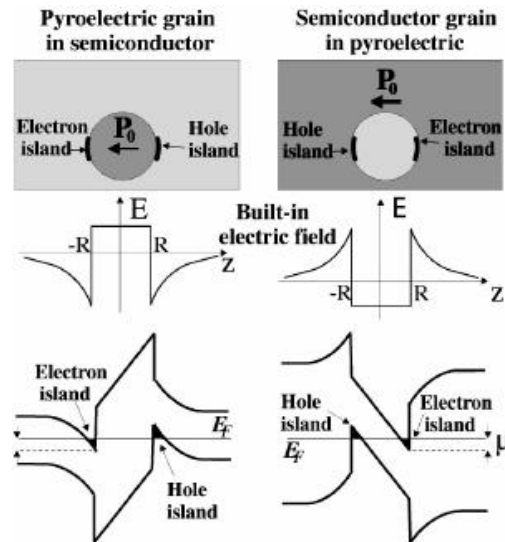


Fig. 5. Two types of pyroelectric/semiconductor structures with 2D electron and hole moveable islands. [25]

## 5. SURFACE ACOUSTIC WAVE AND ACOUSTOOPTIC DEVICES

Strong piezoelectric effects in AlN/GaN/InN-based materials make them suitable for applications in visible-

ultraviolet spectral range light control devices, such as acousto-optic modulators, deflectors, and tunable filters. A very high acoustic velocity in AlN makes this material especially promising for SAW applications in a high frequency electronic signal processing, in particular, for signal filtering and delay. The recent development of gallium nitride based electronics and opto-electronics and the achievements in optical waveguiding and surface acoustic wave propagation in GaN epitaxial layers open the way for the development of integrated acousto-opto-electronic circuits. [26]

The GaN-based SAW sensor for optical radiation with a wavelength up to 365 nm was demonstrated. [27] (Fig. 6)

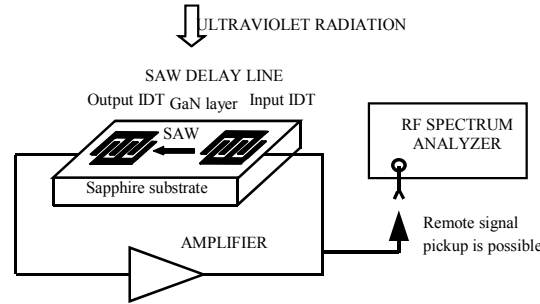


Fig. 6: Schematic diagram of UV-sensor based on SAW delay-line oscillator [27]

Such aluminum-gallium nitride based sensors allow for the adjustment of the cutoff wavelength by varying the compound composition and, hence, the bandgap, which extends the capabilities of SAW-based visible-blind and solar-blind UV photodetectors.

## 6. GaN-BASED HFETs

Achieved output powers of 30 W/mm at 10 GHz demonstrate a great potential of GaN-based HFETs for microwave applications. However, many problems related to gate leakage, gate lag and current collapse, poor reliability and yield still have to be solved. Some of the proposed solutions include strain energy band engineering, new approach to epitaxial growth called Migration Enhanced MOCVD [28], insulated gate design [29], and field plate engineering [19]. AlGaIn/GaN Metal Oxide Semiconductor Heterostructure Field Effect Transistors (MOSHFETs) have been proposed as an alternative to conventional AlGaIn/GaN Heterostructure Field Effect Transistor (HFET). [29] The devices were grown on sapphire and 4H-SiC substrates. The MOSHFETs have a much larger dynamic range, a six orders of magnitude smaller leakage current, and comparable or smaller 1/f noise. Hence, the contribution of the SiO<sub>2</sub>/AlGaIn interface to low-frequency noise is negligible, which confirms a high quality of this interface. Recently, switching applications of MOSHFET technology have been demonstrated as well. [30]

## 7. AlGaIn-BASED UV LEDs

GaN-based UV LEDs will find applications in bio-agents detection, water and air purification, food sterilization, UV curing, fire detection, non-line-of-sight short range communications, and in biomedical systems. Basic designs of GaN based UV LEDs use either sapphire or SiC substrate and rely on the emission through the sapphire substrate or on the edge emission, respectively.

0.1 um p-GaN
p-AlGaIn grading to x=15%
p-AlGaIn x=0.4 blocking
3 MQW for 340 nm emitting
3 um thick n-AlGaIn x=26%
AlN/AlGaIn SLs
AlN buffer
c-plane sapphire

Figure 7. Device structure of 340 nm LED.

SiC substrates are inferior in terms of the light extraction but have a much larger thermal conductivity than sapphire. AlN bulk substrates combine both advantages and they are “native” substrate for AlGaN alloys with a high molar fraction of Al. Recently, we reported on high-efficiency 280 nm LEDs [31] and on 265 nm LEDs [32] with continuous-wave (CW) powers in excess of 1 mW. This progress has been achieved by using AlN/AlGaN strain-defects management superlattices [33] for defect filtration and by improved materials growth using Migration Enhanced Metalorganic Chemical Vapor Deposition (MEMOCVD).[34] Fig. 7 shows a typical deep UV structure.

Further improvements will have to rely on better understanding of device physics, including electron and hole transport, injection, radiative and non-radiative recombination, polarization effects, and the low frequency noise.

## 8. THz PLASMA WAVE ELECTRONICS

Transistors with nanometer critical feature sizes, such as HBTs and HEMTs, relying on ballistic transport in semiconductors with small electron effective masses and on innovative designs minimizing parasitics, are penetrating the subterahertz range, still being dominated by two terminal devices. New ideas of using plasma resonances for tunable detection and emission of terahertz radiation are being explored. Plasma effects in polarization induced electrons and holes in 2D and 1D pyroelectric heterostructures hold promise of an active THz medium. The development of tunable solid state monolithically integrated THz sources and detectors based on these approaches will enable many applications of THz radiation ranging from detection of biological hazardous agents, and explosives, and mines to medical diagnostics, contactless in-situ testing of integrated circuits, and applications in spectroscopy, radio astronomy and environmental control.

A short field effect transistor made from a material with a high mobility acts as a resonant cavity for the surface plasma waves. Such transistor could be used as tunable resonant detector of terahertz radiation. Such resonant detection was demonstrated in 0.15 micron AlGaAs/GaAs FETs at 2.5 THz, 1.2 THz, and 600 GHz. When a current flows through a ballistic field effect transistor, the plasma waves should become unstable and lead to the emission of a terahertz or sub-terahertz radiation at the plasma wave frequencies. [35] Hence, a deep submicron transistor operates as a resonant tunable emitter of terahertz radiation when excited by a small DC current. Terahertz and subterahertz emission related to the plasma wave excitation was observed in InGaAs-based and GaN-based Heterostructure Field Effect Transistors.

In GaN materials system, high polar optical phonon energy results in a much higher peak velocity than in GaAs, especially at cryogenic temperatures. This allows for reaching very short transit times at voltages just below saturation and meeting the criterion required for the plasma wave instability. Recently, we reported on the millimeter wave emission of the electromagnetic radiation by a 1.5 micron gate GaN-based HEMT at voltages close to the current saturation voltage and linked this emission to the excitation of plasma waves in the device channel at cryogenic temperatures (see . [36]) Fig. 8 shows the emission spectrum from a 60 nm InGaAs HEMT. [37]

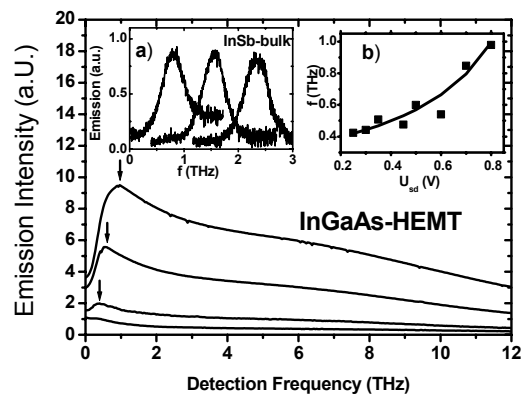


Fig. 8. The spectra of the emission from InGaAs HEMT for different source –drain voltages  $U_{sd}$ . The arrows mark the maxima position for emission at 0.42THz, 0.56THz and 1.0THz –obtained for  $U_{sd}$  0.3V, 0.6V and 0.8V correspondingly. Insert a) shows the calibration curves - cyclotron emission from the InSb bulk emitter as analyzed by the InSb detector. The different maxima correspond to the emitter placed in different magnetic fields: 0.4T, 0.8T and 1.2T (from left to right). Insert b) represents the resonant frequencies of the emission from InGaAs HEMT versus source-drain voltage. The continuous line is plotted using the plasma wave theory.

## 10. CONCLUSIONS

New device physics of nitride based materials enables new applications but requires new designs and new modeling approaches. Emerging GaN based devices include pyroelectric and piezoelectric sensors, HFETs, SAW and acousto-optics devices, UV photodetectors, bioelectronic devices, green, blue and UV LEDs, and THz plasma wave electronics devices. Future progress depends on achieving still better materials quality and on a deeper understanding of new and complicated device physics.

## REFERENCES

- 
- [1] W. C. Johnson, J.B. Parsons, and M. C. Crew, *J. Phys. Chem.* 36, 2651, 1932
  - [2] A. G. Fischer, *Solid-State Electronics*. 2, 231, 1961
  - [3] G. V. Samsonov, *Nonmetallic Nitrides*, in Russian, Naukova Dumka, Kiev (1969)
  - [4] J. I. Pankove, E. A. Miller, and J. E. Berkeyheiser, *J. Lumin.* 4, 63 (1971)
  - [5] M. Asif Khan, A. Bhattarai, J. N. Kuznia and D. T. Olson, *Appl. Phys. Lett.* 63, 1214 (1993)
  - [6] A. Bykhovski, B. Gelmont, and M. S. Shur, *J. Appl. Phys.* 74, p. 6734-6739 (1993)
  - [7] S. Nakamura, M. Senoh, S. Nagahama, N. Iwasa, T. Yamada, T. Matsushita, Y. Sugimoto, and H. Kiyoki, *Appl. Phys. Lett.*, 69, 1477 (1996)
  - [8] M. S. Shur, A. D. Bykhovski, R. Gaska, and A. Khan, *GaN-based Pyroelectronics and Piezoelectronics*, in *Handbook of Thin Film Devices, Volume 1: Hetero-structures for High Performance Devices*, Edited by Colin E.C. Wood, Handbook edited by Maurice H. Francombe, pp. 299-339, Academic Press, San Diego, 2000
  - [9] M. S. Shur and A. Zukauskas, Editors, *UV Solid-State Light Emitters and Detectors. Proc. NATO ARW, Series II, Vol. 144*, Kluwer, Dordrecht, 2004
  - [10] M. S. Shur and R. Davis, *GaN-based Materials and Devices: Growth, Fabrication, Characterization and Performance*, World Scientific, 2004
  - [11] D. Ciplys, M. S. Shur, R. Gaska, R. Rimeika, A. Sereika, J. Deng, J. Yang, M. Asif Khan, "GaN-based acoustic wave devices for optoelectronic applications", in *Proceedings of the First International Symposium "Integrated Optoelectronics,"* Proceedings Volume 2002-4, pp. 119-138, Electrochemical Society, Pennington, NJ 08534-2839 (2002)
  - [12] Y. Deng, R. Kersting, J. Xu, R. Ascazubi, X. C. Zhang, M. S. Shur, R. Gaska, G. S. Simin and M. A. Khan, and V. Ryzhii, *Appl. Phys. Lett.* Vol. 84, No 15, pp. 70-72, 2004
  - [13] M. S. Shur, B. Gelmont, and M. A. Khan, *High Electron Mobility in Two-Dimensional Electrons Gas in AlGaIn/GaN Heterostructures and in Bulk GaN*, *J. Electronic Materials*, Vol. 25, No. 5, pp. 777-785 May (1996)
  - [14] B. L. Gelmont, M. S. Shur, and M. Stroschio, *Two-Region Model of High Field Electron Transport in GaN*, *Proceedings of ISDRS-97*, pp. 389-392, Charlottesville, VA, Dec. (1997); B. L. Gelmont, M. S. Shur, and M. Stroschio, *Analytical Theory of Electron Mobility and Drift Velocity in GaN*, *Mat. Res. Soc. Proc. Vol. 449*, pp. 609-614 (1997)
  - [15] A. Dmitriev, V. Kachorovskii, M. S. Shur, and M. Stroschio, *Electron Runaway and Negative Differential Mobility in Two Dimensional Electron or Hole Gas in Elementary Semiconductors*, *Solid State Comm.*, Vol: 113, Issue: 10, pp. 565-568, February 15, 2000
  - [16] A. Dmitriev, V. Kachorovskii, M. S. Shur, and M. Stroschio, *Electron Drift Velocity of Two Dimensional Electron Gas in Compound Semiconductors*, *International Journal of High Speed Electronics and Systems*, Invited, Volume 10, No 1, pp. 103-110, March 2000
  - [17] B. E. Foutz, L. F. Eastman, S. K. O'Leary, M. S. Shur, and U. V. Bhapkar, *Velocity overshoot and ballistic transport in indium nitride*, *Mat. Res. Soc. Proc. Vol. 482*, pp. 821-825 (1998)
  - [18] M. S. Shur and M. Dyakonov, *Two-Dimensional Electrons in Field Effect Transistors*, *International Journal of High Speed Electronics and Systems*, Vol. 9, No. 1, pp. 65-99, March (1998)
  - [19] Y. F. Wu, A. Saxler, M. Moore, P. Smith, S. Sheppard, P. M. Chavarkar, T. Wisleder, U. K. Mishra, and P. Parikh, *IEEE Electron Device Lett.*, vol. 25, pp. 117-119, Mar. 2004.
  - [20] A.D. Bykhovski, V.V. Kaminski, M.S. Shur, Q.C. Chen, and M.A. Khan, *Appl. Phys. Lett.* 68(6), 818-820, 1996
  - [21] J. S. Shor, L. Bemis, A. D. Kurtz, *IEEE Trans. Electron Dev.* 41(5), 661-665, 1994
  - [22] A. Sagar, *Phys. Rev.* 112, 1533, 1958
  - [23] A. D. Bykhovski, V. V. Kaminski, M. S. Shur, Q. C. Chen, and M. A. Khan, *Appl. Phys. Lett.*, 69, 3254, 1996
  - [24] V. Yu. Kachorovskii and M.S. Shur, *Appl. Phys. Lett.* 86, 12101, 2005
  - [25] V. Yu. Kachorovskii and M.S. Shur, *Appl. Phys. Lett.* 84, 2340-2342 March 29 (2004)
  - [26] D. Ciplys, M. S. Shur, R. Gaska, R. Rimeika, A. Sereika, J. Deng, J. Yang, M. Asif Khan, "GaN-based acoustic wave devices for optoelectronic applications", in *Proceedings of the First International Symposium "Integrated Optoelectronics,"* Vol. 2002-4, pp. 119-138, ECS (2002)
  - [27] D. Ciplys, R. Rimeika, M. S. Shur, S. Romyantsev, R. Gaska, A. Sereika, J. Yang, and M. Asif Khan, "Response of GaN-based surface acoustic wave oscillator to ultraviolet radiation", *Appl. Phys. Lett.*, vol. 80, nr. 11, p. 2020-2022, 2002.
  - [28] Q. Fareed, R. Gaska, and M. S. Shur, *ISDRS Digest, FA1-03*, pp 402-403, Washington DC (2003)
  - [29] G. Simin and M. Asif Khan, M. S. Shur, and R. Gaska, in *GaN-based Materials and Devices: Growth, Fabrication, Characterization and Performance*, M. S. Shur and R. Davis, Editors, World Scientific, 2004
  - [30] G. Simin and M. Asif Khan, M. S. Shur, R. Gaska, *High-power switching using III-Nitride Metal-Oxide Semiconductor Heterostructures*, *International Journal of High Speed Electronics and Systems*, to be published

- 
- [31] J. P. Zhang, X. Hu, Y. Bilenko, J. Deng, A. Lunev, M. S. Shur, R. Gaska, M. Shatalov, J. W. Yang, M. A. Khan, *Appl. Phys. Lett.*, Vol. 85, pp. 5532-5534, 2004
- [32] Y. Bilenko, A. Lunev, X. Hu, J. Deng, T. M Katona, J. Zhang, R. Gaska, M. S Shur, W. Sun, V. Adivarahan, M. Shatalov, and A. Khan, *JJAP, Express Letter*, Vol. 44, No. 3, pp. L98-L100, 2005
- <sup>33</sup> J. P. Zhang, H. M. Wang, M. E. Gaevski, C. Q. Chen, Q. Fareed, J. W. Yang, G. Simin, M. Asif Khan. *Appl. Phys. Lett.* 80, 3542 (2002)
- <sup>34</sup> J. P. Zhang, Q. Fareed, R. Gaska, G. Tamulaitis, M. S. Shur, and M. Asif Khan, Migration Enhanced MOCVD (MEMOCVD) of High Quality III-Nitride Heterostructures and Superlattices, *phys. stat. sol. (c)* submitted for publication
- [35] M. Dyakonov and M.S. Shur, *Phys. Rev. Lett.* 71, 2465 (1993) M. Dyakonov and M. S. Shur, *IEEE Trans. on Elec. Dev.* 43, 380, (1996)
- [36] Y. Deng, R. Kersting, J. Xu, R. Ascazubi, X. C. Zhang, M. S. Shur, R. Gaska, G. S. Simin and M. A. Khan, and V. Ryzhii, *Appl. Phys. Lett.* Vol. 84, No 15, pp. 70-72, January 2004
- [37] W. Knap, J. Lusakowski, T. Parenty, S. Bollaert, A. Cappy, V. Popov, and M. S. Shur, Emission of terahertz radiation by plasma waves in 60 nm AlInAs/InGaAs high electron mobility transistors, *Appl. Phys. Lett.* 84, No 13, 2331-2333, March 29 (2004)